59. Quark Masses

Updated August 2019 by A.V. Manohar (UC, San Diego), L.P. Lellouch (CNRS & Aix-Marseille U.), and R.M. Barnett (LBNL).

59.1. Introduction

This note discusses some of the theoretical issues relevant for the determination of quark masses, which are fundamental parameters of the Standard Model of particle physics. Unlike the leptons, quarks are confined inside hadrons and are not observed as physical particles. Quark masses therefore cannot be measured directly, but must be determined indirectly through their influence on hadronic properties. Although one often speaks loosely of quark masses as one would of the mass of the electron or muon, any quantitative statement about the value of a quark mass must make careful reference to the particular theoretical framework that is used to define it. It is important to keep this *scheme dependence* in mind when using the quark mass values tabulated in the data listings.

Historically, the first determinations of quark masses were performed using quark models. These are usually called constituent quark masses and are of order 350 MeV for the u and d quarks. Constituent quark masses model the effects of dynamical chiral symmetry breaking discussed below, and are not directly related to the quark mass parameters m_q of the QCD Lagrangian of Eq. (59.1). The resulting masses only make sense in the limited context of a particular quark model, and cannot be related to the quark mass parameters, m_q, of the Standard Model. In order to discuss quark masses at a fundamental level, definitions based on quantum field theory must be used, and the purpose of this note is to discuss these definitions and the corresponding determinations of the values of the masses.

59.2. Mass parameters and the QCD Lagrangian

The QCD [1] Lagrangian is

$$\mathcal{L} = \sum_{q=u,d,s,\ldots,t} \overline{q}\left(i\not{D} - m_q\right) q - \frac{1}{2}\mathrm{tr}\, G_{\mu\nu}G^{\mu\nu}, \tag{59.1}$$

where the sum runs over the quark flavors u, d, s, c, b and t. $\not{D} = \left(\partial_\mu - igA_\mu\right)\gamma^\mu$ is the gauge covariant derivative, A_μ is the $su(3)$-valued gluon field, $G_{\mu\nu} = \dfrac{i}{g}[D_\mu, D_\nu]$ is the gluon field strength, m_q is the mass parameter of quark flavor q, and q is the quark Dirac field. After renormalization, the QCD Lagrangian Eq. (59.1) gives finite values for physical quantities, such as scattering amplitudes. Renormalization is a procedure that invokes a subtraction scheme to render the amplitudes finite, and requires the introduction of a dimensionful scale parameter μ. The mass parameters in the QCD Lagrangian Eq. (59.1) depend on the renormalization scheme used to define the theory, and also on the scale parameter μ. The most commonly used renormalization scheme for QCD perturbation theory is the $\overline{\mathrm{MS}}$ scheme.

The QCD Lagrangian has a chiral symmetry in the limit that the quark masses vanish. This symmetry is spontaneously broken by dynamical chiral symmetry breaking, and explicitly broken by the quark masses. The non-perturbative scale of dynamical chiral

symmetry breaking, Λ_χ, is around 1 GeV [2]. It is conventional to call quarks heavy if $m_q > \Lambda_\chi$, so that explicit chiral symmetry breaking dominates (c, b, and t quarks are heavy), and light if $m_q < \Lambda_\chi$, so that spontaneous chiral symmetry breaking dominates (the u and d are light and the s is considered to be light when using $\mathrm{SU}(3)_L \times \mathrm{SU}(3)_R$ chiral perturbation theory). The determination of light- and heavy-quark masses is considered separately in Sec. 59.4 and Sec. 59.5 below.

At high energies or short distances, non-perturbative effects, such as chiral symmetry breaking, become small and one can, in principle, determine quark masses by analyzing mass-dependent effects using QCD perturbation theory. Such computations are conventionally performed using the $\overline{\mathrm{MS}}$ scheme at a scale $\mu \gg \Lambda_\chi$, and give the $\overline{\mathrm{MS}}$ "running" mass $\overline{m}(\mu)$. We use the $\overline{\mathrm{MS}}$ scheme when reporting quark masses; one can readily convert these values into other schemes using perturbation theory.

The μ dependence of $\overline{m}(\mu)$ at short distances can be calculated using the renormalization group (RG) equation,

$$\mu^2 \frac{\mathrm{d}\overline{m}\,(\mu)}{\mathrm{d}\mu^2} = -\gamma(\overline{\alpha}_s\,(\mu))\;\overline{m}\,(\mu)\,, \tag{59.2}$$

where γ is the anomalous dimension which is now known to four-loop order in perturbation theory [3,4]. $\overline{\alpha}_s$ is the coupling constant [1] in the $\overline{\mathrm{MS}}$ scheme. Defining the expansion coefficients γ_r by

$$\gamma\,(\overline{\alpha}_s) \equiv \sum_{r=1}^{\infty} \gamma_r \left(\frac{\overline{\alpha}_s}{4\pi}\right)^r,$$

the first four coefficients are given by

$$\begin{aligned}
\gamma_1 &= 4,\\
\gamma_2 &= \frac{202}{3} - \frac{20N_L}{9},\\
\gamma_3 &= 1249 + \left(-\frac{2216}{27} - \frac{160}{3}\zeta\,(3)\right) N_L - \frac{140}{81}N_L^2,\\
\gamma_4 &= \frac{4603055}{162} + \frac{135680}{27}\zeta\,(3) - 8800\zeta\,(5)\\
&\quad + \left(-\frac{91723}{27} - \frac{34192}{9}\zeta\,(3) + 880\zeta\,(4) + \frac{18400}{9}\zeta\,(5)\right) N_L\\
&\quad + \left(\frac{5242}{243} + \frac{800}{9}\zeta\,(3) - \frac{160}{3}\zeta\,(4)\right) N_L^2\\
&\quad + \left(-\frac{332}{243} + \frac{64}{27}\zeta\,(3)\right) N_L^3,
\end{aligned}$$

where N_L is the number of active light quark flavors at the scale μ, i.e. flavors with masses $< \mu$, and ζ is the Riemann zeta function ($\zeta(3) \simeq 1.2020569$, $\zeta(4) \simeq 1.0823232$, and $\zeta(5) \simeq 1.0369278$). Eq. (59.2) must be solved in conjunction with the RG equation for $\overline{\alpha}_s(\mu)$ given in [1]. In addition, as the renormalization scale crosses quark mass thresholds one needs to match the scale dependence of $\overline{m}$ below and above the threshold. There are finite threshold corrections; the necessary formulae can be found in Ref. [5].

59.3. Lattice QCD

The use of lattice QCD calculations for *ab initio* determinations of the fundamental parameters of QCD, including the coupling constant and quark masses (except for the top-quark mass) is a very active area of research (see the review on Lattice Quantum Chromodynamics in this *Review*). Here we only briefly recall those features which are required for the determination of quark masses. In order to determine the lattice spacing (a, i.e. the distance between neighboring points of the lattice) and quark masses, one computes a convenient and appropriate set of physical quantities (frequently chosen to be a set of hadronic masses) for a variety of input values of the quark masses in units of the lattice spacing. These input quark masses are then tuned to their true (physical) values by requiring that the calculation correctly reproduces the set of physical quantities being used for the calibration.

The resulting values of the quark masses are bare quark masses, corresponding to a particular discretization of QCD and with the lattice spacing as the ultraviolet cut-off. In order for these results to be useful in phenomenological applications, it is necessary to relate them to renormalized masses defined in some standard renormalization scheme such as $\overline{\rm MS}$. Provided that both the ultraviolet cut-off a^{-1} and the renormalization scale μ are much greater than $\Lambda_{\rm QCD}$, the bare and renormalized masses can be related in perturbation theory. However, in order to avoid uncertainties due to the unknown higher-order coefficients in lattice perturbation theory, most results obtained recently use *non-perturbative renormalization* to relate the bare masses to those defined in renormalization schemes which can be realized directly in lattice QCD (e.g. those obtained from quark and gluon Green functions at specified momenta in the Landau gauge [6] or those defined using finite-volume techniques and the Schrödinger functional [7], but not $\overline{\rm MS}$ that is only defined for dimensional regularization). These methods require $\mu \gg \Lambda_{\rm QCD}$ so that unwanted (non-perturbative) corrections proportional to inverse powers of μ, which appear in some approaches, remain small corrections that can be identified and removed. This condition is also necessary so that matching to other schemes can be performed reliably in perturbation theory. Moreover, these methods require $a^{-1} \gg \mu$ so that cutoff effects are small enough to be extrapolated away. Thus, the calculations are repeated for finer and finer lattices spacings and the continuum limit, $a \to 0$, of these non-perturbatively renormalized masses is taken to eliminate all cutoff effects. The conversion to the $\overline{\rm MS}$ scheme is then performed using continuum perturbation theory, which is more readily obtained to higher orders and is usually better behaved than its lattice counterpart.

It is important to note that the issues surrounding the renormalization of quark masses disappear when considering pairwise ratios of these masses (up to electromagnetic effects

for quarks of different charge, which are negligible compared to other uncertainties at present). Indeed, if the same scheme and scale are implemented, QCD renormalization factors are identical for all quark flavors, and these factors therefore cancel exactly in quark-mass ratios. In particular, this means that these ratios are scheme and scale independent. Moreover, these ratios suffer little from the uncertainties in the determination of the lattice scale because they are dimensionless. Thus, quark-mass ratios are typically determined with significantly higher precision using lattice QCD than are the individual masses.

The determination of quark masses using lattice simulations is well established and the current emphasis is on the reduction and control of the systematic uncertainties. With improved algorithms and access to more powerful computing resources, the precision of the results has improved immensely in recent years. Vacuum polarization effects are included with $N_f = 2$, $2+1$ or $N_f = 2+1+1$ flavors of sea quarks. The number 2 here indicates that the up and down quarks are degenerate. Simulations with $2+1$ and $2+1+1$ flavors represent controlled approximations to physical QCD at the low energies considered for quark mass determinations, up to corrections of $O((\Lambda_{\rm QCD}/m_c)^2/N_c)$ and $O((\Lambda_{\rm QCD}/m_b)^2/N_c)$, respectively. This is not the case for simulations with $N_f = 2$ or in which vacuum polarization effects are completely neglected (this is the so-called *quenched* approximation) and results obtained in such frameworks will not enter the discussion here.

Particularly pleasing is the observation that different formulations of lattice QCD, with different systematic uncertainties, yield results which are largely consistent with each other. This gives us broad confidence in the estimates of the systematic errors. As the precision of the results approaches (or even exceeds in some cases) 1%, isospin breaking effects, including electromagnetic corrections need to be included and this is beginning to be done as will be discussed below. In particular, a reliable estimate of these effects is required for determining the individual u and d quark masses.

Members of the lattice QCD community have organized a Flavour Lattice Averaging Group (FLAG) which critically reviews quantities computed in lattice QCD relevant to flavor physics, including the determination of quark masses, against stated quality criteria and presents its view of the current status of the results. The latest edition reviews lattice results published before September 30th 2018 [8]. Since that deadline, only a single lattice determination of quark masses has appeared [9]. It is a computation of m_c and m_b in $N_f = 2+1$ QCD, based on the method of Euclidean-time moments of pseudoscalar, two-point functions of $c\overline{c}$ quark-bilinear operators described below. Its results are fully consistent with the lattice averages quoted later.

59.4. Light quarks

In this section we review the determination of the masses of the light quarks u, d and s from lattice simulations and then discuss the consequences of the approximate chiral symmetry.

59.4.1. *Lattice QCD results* :

The most reliable determinations of the strange quark mass m_s and of the average of the up and down quark masses $m_{ud} = (m_u + m_d)/2$ are obtained from lattice simulations. As explained in Sec. 59.3 above, the simulations are generally performed with degenerate up and down quarks ($m_u = m_d$) and so it is the average which is obtained directly from the computations. Below we discuss the derivation of m_u and m_d separately, but we start by briefly presenting our estimate of the current status of the latest lattice results in the isospin symmetric limit. The FLAG Review [8] bases its summary numbers for these quark masses largely on references [10–15] for $N_f = 2+1$ and references [16–19] for $N_f = 2+1+1$ flavors of sea quarks, which its authors consider to have the most reliable estimates of the systematic uncertainties. For $N_f = 2+1$ flavors, they quote $\overline{m}_{ud} = (3.364 \pm 0.041)\,\text{MeV}$, $\overline{m}_s = (92.03 \pm 0.88)\,\text{MeV}$ and $(\overline{m}_s/\overline{m}_{ud}) = 27.42 \pm 0.12$. These numbers are $\overline{m}_{ud} = (3.410 \pm 0.043)\,\text{MeV}$, $\overline{m}_s = (93.44 \pm 0.68)\,\text{MeV}$ and $(\overline{m}_s/\overline{m}_{ud}) = 27.23 \pm 0.10$ for $N_f = 2+1+1$ simulations. The masses are given in the $\overline{\text{MS}}$ scheme at a renormalization scale of 2 GeV. Because of the systematic errors, these results are not simply the combinations of all the results in quadrature, but include a judgement of the remaining uncertainties. Since the different collaborations use different formulations of lattice QCD, the (relatively small) variations of the results between the groups provides important information about the reliability of the estimates.

Despite being reported in the $\overline{\text{MS}}$ scheme at a renormalization scale of 2 GeV, the results for $\overline{m}_{ud}$ and $\overline{m}_s$ in the two frameworks differ in their renormalization schemes, since $N_f = 2+1$ results are renormalized with $N_L = 3$ and $N_f = 2+1+1$ ones with $N_L = 4$. Thus, for a comparison, in principle one should convert the results to the same scheme. This is not the case for $(\overline{m}_s/\overline{m}_{ud})$, where renormalization factors cancel. The conversion of the $N_f = 2+1$ results to the $N_L = 4$ scheme can be performed, for instance, by running them down to the charm threshold in the $N_L = 3$ theory, matching the results to the $N_L = 4$ theory and running them back up to 2 GeV in that theory. Such a conversion, however, leads to shifts in the values of the quark masses that are well within the quoted errors. Thus, we choose simply to average the results from the two frameworks, yielding as a final lattice QCD estimate in the $\overline{\text{MS}}$ scheme at $\mu = 2\,\text{GeV}$ in the $N_L = 4$ theory:

$$\overline{m}_{ud} = (3.39 \pm 0.04)\,\text{MeV} \tag{59.3}$$

$$\overline{m}_s = (92.9 \pm 0.7)\,\text{MeV}, \tag{59.4}$$

and

$$\frac{\overline{m}_s}{\overline{m}_{ud}} = 27.37 \pm 0.10. \tag{59.5}$$

where the error bars encompass statistical and systematic errors combined in quadrature. In performing these averages, the only slight tension found is in $\overline{m}_s$ where the weighted

average carries a $\chi^2/dof = 1.6$, used to increase the error by the usual $\sqrt{\chi^2/dof}$ scale factor. Note also that we do not allow the errors to become smaller than those on the individual averages because of possible common systematics.

To obtain the individual values of $\overline{m}_u$ and $\overline{m}_d$ requires the introduction of isospin breaking effects, including electromagnetism. This is now being done completely using lattice field theory, albeit neglecting electromagnetic effects in the sea in most cases (see the computation of the neutron-proton mass splitting [20] for an exception). The effect of this neglect on the u and d quark masses has been estimated in [21], to induce a contribution to the uncertainty that ranges from about 3% in $\overline{m}_u/\overline{m}_d$ to less than 1% in $\overline{m}_d$. FLAG has reviewed these quantities in [8]. Again, they separate results obtained from $N_f = 2+1$ and $N_f = 2+1+1$ simulations. For the former, their final averages are the results of [21], and for the latter, those of [22]. Thus, for $N_f = 2+1$ they quote $\overline{m}_u = 2.27(9)\,\text{MeV}$, $\overline{m}_d = 4.67(9)\,\text{MeV}$, $(\overline{m}_u/\overline{m}_d) = 0.485(19)$ and, for $N_f = 2+1+1$, $\overline{m}_u = 2.50(17)\,\text{MeV}$, $\overline{m}_d = 4.88(20)\,\text{MeV}$, $(\overline{m}_u/\overline{m}_d) = 0.513(31)$. As for the light quark masses in the isospin limit, we average the results obtained with different numbers of sea-quark flavors. Here, only the $\overline{m}_u$ average has a $\chi^2/dof = 1.4 > 1$, and its error is thus appropriately scaled. Again, we do not allow the errors to become smaller than those on the individual averages because of possible common systematics. Thus, we give as a final lattice QCD estimate in the $\overline{\text{MS}}$ scheme at $\mu = 2\,\text{GeV}$ in the $N_L = 4$ theory:

$$\overline{m}_u = 2.32(10)\,\text{MeV},\ \overline{m}_d = 4.71(9)\,\text{MeV},\ \frac{\overline{m}_u}{\overline{m}_d} = 0.493(19). \tag{59.6}$$

Of particular importance is the fact that $m_u \neq 0$ to more than 20 standard deviations, since there would have been no strong CP problem had m_u been equal to zero.

The results for the light quark masses given in the listings are dominated by the lattice values, since most continuum extractions have larger uncertainties.

59.4.2. *Chiral Perturbation Theory* :

For light quarks, one can use the techniques of chiral perturbation theory [23–25] to extract quark mass ratios. The mass term for light quarks in the QCD Lagrangian is

$$\overline{\Psi} M \Psi = \overline{\Psi}_L M \Psi_R + \overline{\Psi}_R M^\dagger \Psi_L, \tag{59.7}$$

where M is the light quark mass matrix,

$$M = \begin{pmatrix} m_u & 0 & 0 \\ 0 & m_d & 0 \\ 0 & 0 & m_s \end{pmatrix}, \tag{59.8}$$

$\Psi = (u, d, s)$, and L and R are the left- and right-chiral components of Ψ given by $\Psi_{L,R} = P_{L,R}\Psi$, $P_L = (1-\gamma_5)/2$, $P_R = (1+\gamma_5)/2$. The mass term is the only term in the QCD Lagrangian that mixes left- and right-handed quarks. In the limit $M \to 0$, there is an independent SU(3)×U(1) flavor symmetry for the left- and right-handed quarks. The vector $U(1)$ symmetry is baryon number; the axial $U(1)$ symmetry of the

classical theory is broken in the quantum theory due to the anomaly. The remaining $G_\chi = \mathrm{SU}(3)_L \times \mathrm{SU}(3)_R$ chiral symmetry of the QCD Lagrangian is spontaneously broken to $\mathrm{SU}(3)_V$, which, in the limit $M \to 0$, leads to eight massless Goldstone bosons, the π's, K's, and η.

The symmetry G_χ is only an approximate symmetry, since it is explicitly broken by the quark mass matrix M. The Goldstone bosons acquire masses which can be computed in a systematic expansion in M, in terms of low-energy constants, which are unknown non-perturbative parameters of the effective theory, and are not fixed by the symmetries. One treats the quark mass matrix M as an external field that transforms under G_χ as $M \to LMR^\dagger$, where $\Psi_L \to L\Psi_L$ and $\Psi_R \to R\Psi_R$ are the $\mathrm{SU}(3)_L$ and $\mathrm{SU}(3)_R$ transformations, and writes down the most general Lagrangian invariant under G_χ. Then one sets M to its given constant value Eq. (59.8), which implements the symmetry breaking. To first order in M one finds that [26]

$$\begin{aligned} m_{\pi^0}^2 =& B\,(m_u + m_d)\,, \\ m_{\pi^\pm}^2 =& B\,(m_u + m_d) + \Delta_{\mathrm{em}}, \\ m_{K^0}^2 =& m_{\overline{K}^0}^2 = B\,(m_d + m_s)\,, \\ m_{K^\pm}^2 =& B\,(m_u + m_s) + \Delta_{\mathrm{em}}, \\ m_\eta^2 =& \frac{1}{3} B\,(m_u + m_d + 4m_s)\,, \end{aligned} \tag{59.9}$$

with two unknown constants B and Δ_{em}, the electromagnetic mass difference. From Eq. (59.9), one can determine the quark mass ratios [26]

$$\begin{aligned} \frac{m_u}{m_d} =& \frac{2m_{\pi^0}^2 - m_{\pi^+}^2 + m_{K^+}^2 - m_{K^0}^2}{m_{K^0}^2 - m_{K^+}^2 + m_{\pi^+}^2} = 0.56, \\ \frac{m_s}{m_d} =& \frac{m_{K^0}^2 + m_{K^+}^2 - m_{\pi^+}^2}{m_{K^0}^2 + m_{\pi^+}^2 - m_{K^+}^2} = 20.2, \end{aligned} \tag{59.10}$$

to lowest order in chiral perturbation theory, with an error which will be estimated below. Since the mass ratios extracted using chiral perturbation theory use the symmetry transformation property of M under the chiral symmetry G_χ, it is important to use a renormalization scheme for QCD that does not change this transformation law. Any mass independent subtraction scheme such as $\overline{\mathrm{MS}}$ is suitable. The ratios of quark masses are scale independent in such a scheme (up to electromagnetic corrections), and Eq. (59.10) can be taken to be the ratio of $\overline{\mathrm{MS}}$ masses. Chiral perturbation theory cannot determine the overall scale of the quark masses, since it uses only the symmetry properties of M, and any multiple of M has the same G_χ transformation law as M.

Chiral perturbation theory is a systematic expansion in powers of the light quark masses. The typical expansion parameter is $m_K^2/\Lambda_\chi^2 \sim 0.25$ if one uses SU(3) chiral

symmetry, and $m_\pi^2/\Lambda_\chi^2 \sim 0.02$ if instead one uses SU(2) chiral symmetry. Electromagnetic effects at the few percent level also break SU(2) and SU(3) symmetry. The mass formulæ Eq. (59.9) were derived using SU(3) chiral symmetry, and are expected to have approximately a 25% uncertainty due to second order corrections. This estimate of the uncertainty is consistent with the lattice results summarized in Eq. (59.4) – Eq. (59.5).

There is a subtlety which arises when one tries to determine quark mass ratios at second order in chiral perturbation theory. The second order quark mass term [27]

$$\left(M^\dagger\right)^{-1} \det M^\dagger \tag{59.11}$$

(which can be generated by instantons) transforms in the same way under G_χ as M. Chiral perturbation theory cannot distinguish between M and $(M^\dagger)^{-1} \det M^\dagger$; one can make the replacement $M \to M(\lambda) = M + \lambda M (M^\dagger M)^{-1} \det M^\dagger$ in the chiral Lagrangian,

$$\begin{aligned} M(\lambda) &= \mathrm{diag}\,(m_u(\lambda),\ m_d(\lambda),\ m_s(\lambda)) \\ &= \mathrm{diag}\,(m_u + \lambda m_d m_s,\ m_d + \lambda m_u m_s,\ m_s + \lambda m_u m_d)\,, \end{aligned} \tag{59.12}$$

and leave all observables unchanged.

The combination

$$\left(\frac{m_u}{m_d}\right)^2 + \frac{1}{Q^2}\left(\frac{m_s}{m_d}\right)^2 = 1 \tag{59.13}$$

where

$$Q^2 = \frac{m_s^2 - m_{ud}^2}{m_d^2 - m_u^2}, \qquad m_{ud} = \frac{1}{2}\,(m_u + m_d)\,,$$

is insensitive to the transformation in Eq. (59.12). Eq. (59.13) gives an ellipse in the $m_u/m_d - m_s/m_d$ plane. The ellipse is well-determined by chiral perturbation theory, but the exact location on the ellipse, and the absolute normalization of the quark masses, has larger uncertainties. Q is determined to be 22.1(7) from $\eta \to 3\pi$ decay and the electromagnetic contribution to the $K^+ – K^0$ and $\pi^+ – \pi^0$ mass differences [28]. Lattice QCD collaborations have also reported determinations of Q. Using $N_f = 2 + 1$ simulations, [21] obtains $Q = 23.4(6)$ and [22] determines $Q = 23.8(1.1)$ with $N_f = 2{+}1{+}1$ simulations, which are fully compatible. The $N_f = 2 + 1$ result is about 2 standard deviations larger than the one from phenomenology given above [28]. These values can also be compared to the leading-order result for Q in SU(3) chiral perturbation theory, that can be derived using Eq. (59.9) and the values for the relevant meson masses given in this review. This result also holds to next-to-leading order, thus: $Q \overset{\mathrm{NLO}}{=} 24.3$.

The absolute normalization of the quark masses cannot be determined using chiral perturbation theory. Other methods, such as lattice simulations discussed above, or spectral function sum rules [29,30] for hadronic correlation functions reviewed next, are necessary.

59.4.3. ***Sum rules*** :

Sum rule methods have been used extensively to determine quark masses and for illustration we briefly discuss here their application to hadronic τ decays [31]. Other applications involve very similar techniques.

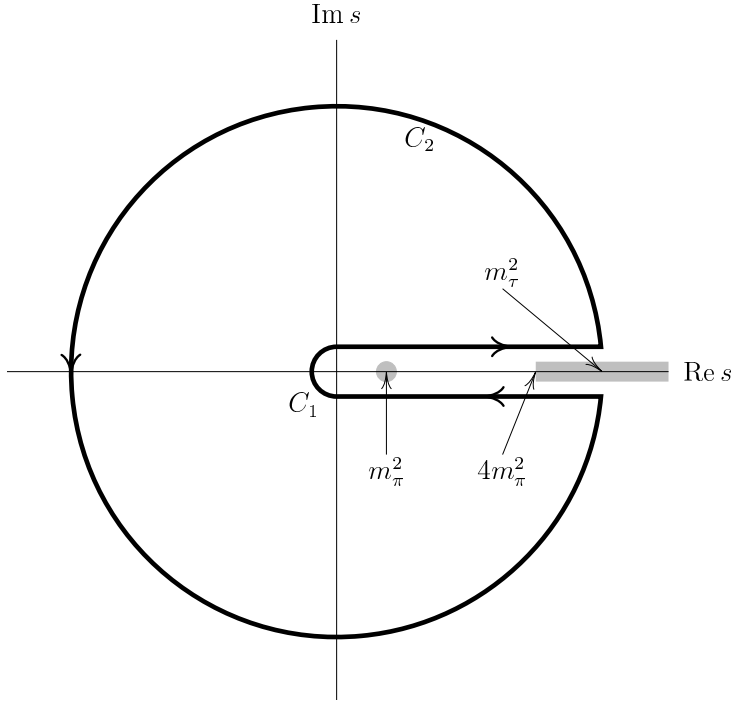

Figure 59.1: The analytic structure of $\Pi(s)$ in the complex s-plane. The contours C_1 and C_2 are the integration contours discussed in the text, and the integral over the closed contour $C_1 + C_2$ vanishes. m_τ^2 has not been drawn to scale; $m_\tau^2 \sim 40(4m_\pi^2)$.

The experimentally measured quantity is R_τ,

$$\frac{\mathrm{d}R_\tau}{\mathrm{d}s} = \frac{\mathrm{d}\Gamma/\mathrm{d}s\left(\tau^- \to \text{hadrons} + \nu_\tau(\gamma)\right)}{\Gamma\left(\tau^- \to e^-\overline{\nu}_e\nu_\tau(\gamma)\right)} \tag{59.14}$$

the hadronic invariant mass spectrum in semihadronic τ decay, normalized to the leptonic τ decay rate. It is useful to define q as the total momentum of the hadronic final state, so $s = q^2$ is the hadronic invariant mass. The total hadronic τ decay rate R_τ is then given by integrating $\mathrm{d}R_\tau/\mathrm{d}s$ over the kinematically allowed range $0 \le s \le M_\tau^2$.

R_τ can be written as

$$\begin{aligned} R_\tau =& 12\pi \int_0^{M_\tau^2} \frac{\mathrm{d}s}{M_\tau^2}\left(1 - \frac{s}{M_\tau^2}\right)^2 \\ & \times \left[\left(1 + 2\frac{s}{M_\tau^2}\right)\mathrm{Im}\,\Pi^T(s) + \mathrm{Im}\,\Pi^L(s)\right] \end{aligned} \tag{59.15}$$

where the hadronic spectral functions $\Pi^{L,T}$ are defined from the time-ordered correlation function of two weak currents ($j^\mu(x)$ and $j^\nu(0)$) by

$$\Pi^{\mu\nu}(q) = i \int \mathrm{d}^4x \; e^{iq\cdot x} \, \langle 0| \, T \left(j^\mu(x) j^\nu(0)^\dagger \right) |0\rangle \,, \tag{59.16}$$

$$\Pi^{\mu\nu}(q) = (-g^{\mu\nu} + q^\mu q^\nu) \, \Pi^T(s) + q^\mu q^\nu \Pi^L(s), \tag{59.17}$$

and the decomposition Eq. (59.17) is the most general possible structure consistent with Lorentz invariance.

By the optical theorem, the imaginary part of $\Pi^{\mu\nu}$ is proportional to the total cross-section for the current to produce all possible states. A detailed analysis including the phase space factors leads to Eq. (59.15). The spectral functions $\Pi^{L,T}(s)$ are analytic in the complex s plane, with singularities along the real axis. There is an isolated pole at $s = m_\pi^2$, and single- and multi-particle singularities for $s \geq 4m_\pi^2$, the two-particle threshold. The discontinuity along the real axis is $\Pi^{L,T}(s + i0^+) - \Pi^{L,T}(s - i0^+) = 2i\mathrm{Im}\ \Pi^{L,T}(s)$. As a result, Eq. (59.15) can be rewritten with the replacement $\mathrm{Im}\ \Pi^{L,T}(s) \to -i\Pi^{L,T}(s)/2$, and the integration being over the contour C_1. Finally, the contour C_1 can be deformed to $-C_2$ without crossing any singularities, and so leaving the integral unchanged, i.e. the integral over the closed contour $C_1 + C_2$ vanishes. One can derive a series of sum rules analogous to Eq. (59.15) by weighting the differential τ hadronic decay rate by different powers of the hadronic invariant mass [32],

$$R_\tau^{kl} = \int_0^{M_\tau^2} \mathrm{d}s \; \left(1 - \frac{s}{M_\tau^2}\right)^k \left(\frac{s}{M_\tau^2}\right)^l \frac{\mathrm{d}R_\tau}{\mathrm{d}s} \tag{59.18}$$

where $\mathrm{d}R_\tau/\mathrm{d}s$ is the hadronic invariant mass distribution in τ decay normalized to the leptonic decay rate. This leads to the final form of the sum rule(s),

$$\begin{aligned} R_\tau^{kl} = & -6\pi i \int_{C_2} \frac{\mathrm{d}s}{M_\tau^2} \left(1 - \frac{s}{M_\tau^2}\right)^{2+k} \left(\frac{s}{M_\tau^2}\right)^l \\ & \times \left[\left(1 + 2\frac{s}{M_\tau^2}\right) \Pi^T(s) + \Pi^L(s) \right]. \end{aligned} \tag{59.19}$$

The manipulations so far are completely rigorous and exact, relying only on the general analytic structure of quantum field theory. The left-hand side of the sum rule Eq. (59.19) is obtained from experiment. The right hand-side can be computed for s far away from any physical cuts using the operator product expansion (OPE) for the time-ordered product of currents in Eq. (59.16), and QCD perturbation theory. The OPE is an expansion for the time-ordered product Eq. (59.16) in a series of local operators, and is an expansion about the $q \to \infty$ limit. It gives $\Pi^{L,T}(s)$ as an expansion in powers of $\alpha_s(s)$ and $\Lambda_{\mathrm{QCD}}^2/s$, and is valid when s is far (in units of Λ_{QCD}^2) from any singularities in the complex s-plane.

The OPE gives $\Pi^{L,T}(s)$ as a series in α_s, quark masses, and various non-perturbative vacuum matrix elements. By computing $\Pi^{L,T}(s)$ theoretically, and comparing with the experimental values of R_τ^{kl}, one determines various parameters such as α_s and the quark masses. The theoretical uncertainties in using Eq. (59.19) arise from neglected higher order corrections (both perturbative and non-perturbative), and because the OPE is no longer valid near the real axis, where $\Pi^{L,T}$ have singularities. The contribution of neglected higher order corrections can be estimated as for any other perturbative computation. The error due to the failure of the OPE is more difficult to estimate. In Eq. (59.19), the OPE fails on the endpoints of C_2 that touch the real axis at $s = M_\tau^2$. The weight factor $(1 - s/M_\tau^2)$ in Eq. (59.19) vanishes at this point, so the importance of the endpoint can be reduced by choosing larger values of k.

Light quark masses are often determined using QCD sum rules [30], which are similar to the τ sum rules. One takes the correlator of two light-quark-bilinear operators (e.g. an axial vector current), as in Eq. (59.16), and computes their Laplace transforms or moments

$$\mathcal{L}_n(\tau) = \int_0^\infty \mathrm{d}s\, s^n\, e^{-\tau s}\, \mathrm{Im}\,\Pi(s), \qquad \mathcal{M}_n(Q^2) = \int_0^\infty \frac{\mathrm{d}s}{(s+Q^2)^n}\, \mathrm{Im}\,\Pi(s)$$

to get Laplace or moment sum rules, respectively. The quark masses are extracted by comparing the theoretical and experimental values of $\mathcal{L}_n(\tau)$ and $\mathcal{M}_n(Q^2)$. Considerable theoretical effort has gone into optimizing n and Q^2 to improve the precision of the resulting light quark masses.

59.5. Heavy quarks

59.5.1. *Continuum approaches and results* :

For heavy quark physics one can exploit the fact that $m_Q \gg \Lambda_{\rm QCD}$ to construct effective theories (m_Q is the mass of the heavy quark Q). The masses and decay rates of hadrons containing a single heavy quark, such as the B and D mesons can be determined using the heavy quark effective theory (HQET) [33]. The theoretical calculations involve radiative corrections computed in perturbation theory with an expansion in $\alpha_s(m_Q)$ and non-perturbative corrections with an expansion in powers of $\Lambda_{\rm QCD}/m_Q$. Due to the asymptotic nature of the QCD perturbation series, the two kinds of corrections are intimately related; an example of this are renormalon effects in the perturbative expansion which are associated with non-perturbative corrections.

Systems containing two heavy quarks such as the Υ or J/Ψ are treated using non-relativistic QCD (NRQCD) [34]. The typical momentum and energy transfers in these systems are $\alpha_s m_Q$, and $\alpha_s^2 m_Q$, respectively, so these bound states are sensitive to scales much smaller than m_Q. However, smeared observables, such as the cross-section for $e^+e^- \to \overline{b}b$ averaged over some range of s that includes several bound state energy levels, are better behaved and only sensitive to scales near m_Q. For this reason, most determinations of the c, b quark masses using perturbative calculations compare smeared observables with experiment [35–37]. The method is similar to that outlined for τ decays.

The current correlator in Eq. (59.16) is the electromagnetic current, and the experimental data is the value of $R(s)$ in the threshold region for $e^+e^- \to Q\overline{Q}$. The theoretical values for the moments are computed using renormalization group improved calculations in non-relativistic QCD.

There are many continuum extractions of the c and b quark masses, some with quoted errors of 10 MeV or smaller. There are systematic effects of comparable size, which are typically not included in these error estimates. Reference [38], for example, shows that even though the error estimate of m_c using the rapid convergence of the α_s perturbation series is only a few MeV, the central value of m_c can differ by a much larger amount depending on which algorithm (all of which are formally equally good) is used to determine m_c from the data. This leads to a systematic error from perturbation theory of around 20 MeV for the c quark and 25 MeV for the b quark. Electromagnetic effects, which also are important at this precision, are often not included. For this reason, we inflate the errors on the continuum extractions of m_c and m_b. The average values of m_c and m_b from continuum determinations are (see Sec. G for the 1S scheme)

$$\overline{m}_c(\overline{m}_c) = (1.280 \pm 0.025)\text{GeV},$$

$$\overline{m}_b(\overline{m}_b) = (4.18 \pm 0.03)\,\text{GeV}, \quad m_b^{1\text{S}} = (4.65 \pm 0.03)\,\text{GeV}.$$

59.5.2. ***Lattice approaches and results*** :

Lattice simulations of QCD lead to discretization errors which are powers of am_Q (modulated by logarithms); the power depends on the formulation of lattice QCD being used and in most cases is quadratic. Clearly these errors can be reduced by performing simulations at smaller lattice spacings, but also by using *improved* discretizations of the theory. Recently, with more powerful computing resources, better algorithms and techniques, it has become possible to perform simulations in the charm quark region and beyond, also decreasing the extrapolation which has to be performed to reach the b-quark.

Traditionally the charm quark mass is obtained by tuning its bare, simulation value to reproduce the physical mass of charmonium mesons or of the D, D_s mesons (requiring a more precise tuning of the light quark masses). This mass can then be renormalized to the $\overline{\text{MS}}$ scheme using the methods discussed for the light quarks.

An alternative approach for obtaining the $\overline{\text{MS}}$ mass from the tuned bare quark mass was proposed in [39]. Euclidean-time moments of pseudoscalar, two-point functions of $c\overline{c}$ quark-bilinear operators can readily be computed on the lattice and extrapolated to the continuum limit where they can be compared to perturbative calculations of the same quantities at 4-loop order. In this way, both the strong coupling constant and the charm quark mass can be determined with remarkably small errors. As this approach uses the same perturbative expressions for two-point correlators as the continuum determinations discussed above, it suffers from similar perturbation-theory, systematic errors. FLAG [8] has reviewed lattice determinations of the charm quark mass obtained using both approaches. The most advanced calculations are performed with $N_f = 2+1+1$ simulations. For these, the quoted average is

$$\overline{m}_c(\overline{m}_c) = 1.280(13)\,\text{GeV},$$

based on the calculations performed in [17,16,40,18,19], in good agreement with the continuum result quoted above, but with a smaller error. It is worth noting that while three [17,18,19] of the four calculations entering this average agree, the fourth [16,40] is about two standard deviations larger, and this is taken into account in the error bar. It should also be remembered that these results were obtained in QCD with exact isospin symmetry, though isospin breaking corrections to the physical inputs, including electromagnetism, are accounted for using phenomenology.

Historically, the main approach to controlling the discretization errors in lattice studies of b quark physics was to perform simulations of effective theories such as HQET and NRQCD. This remains an important technique, both in its own right and in providing additional information for extrapolations from lower masses to the bottom region. Using effective theories, m_b is obtained from what is essentially a computation of the difference of $M_{H_b} - m_b$, where M_{H_b} is the mass of a hadron H_b containing a b-quark. The relative error on m_b is therefore much smaller than that for $M_{H_b} - m_b$. The principal systematic errors are the matching of the effective theories to QCD and the presence of power divergences in a^{-1} in the $1/m_b$ corrections which have to be subtracted numerically. A procedure for performing these subtractions fully non-perturbatively was proposed and implemented for the first time in [41].

The most recent lattice QCD determinations of the b quark mass rely on a variety of approaches, including Euclidean-time moments of correlation functions with [42] or without NRQCD [17] and HQET based interpolations [43,44] or extrapolations [18] from above the charm to the b region. The overall agreement of the results obtained using these very different approaches, which have different systematic errors, is a confirmation that the various groups control these uncertainties. As the range of heavy-quark masses which can be used in numerical simulations increases, results obtained by extrapolating the results to b-physics are becoming ever more reliable (see e.g. [18]) . FLAG's compilation [8] of the above $N_f = 2 + 1 + 1$ results yields

$$\overline{m}_b(\overline{m}_b) = 4.198(12)\,\text{GeV}.$$

Again, this result is compatible with the average value of continuum results, but with a significantly smaller uncertainty.

As explained in Sec. 59.3, ratios of quark masses can have significantly smaller errors than the individual masses if they are computed in the same lattice QCD framework and in the same renormalization scheme at identical scales. This led HPQCD to leverage their precise determination of m_c [39] to determine m_s and m_{ud} [57], through a precise computation of m_c/m_s [57] and of m_s/m_{ud} [58]. This $N_f = 2 + 1$ calculation was updated using $N_f = 2 + 1 + 1$ simulations in [17]. The ratio m_s/m_c was also computed in [15,59] with $N_f = 2 + 1$ simulations and in [16,18] with $N_f = 2 + 1 + 1$ ones. Based on [57,59], FLAG quotes [8] $m_c/m_s = 11.82(16)$ for $N_f = 2+1$, and $m_c/m_s = 11.768(33)$ for $N_f = 2 + 1 + 1$, based on [16,17,18], where a 50% stretch of the combined error was applied due to a tension between the results of [16] and [17]. As a final lattice number we give the $N_f = 2 + 1 + 1$ average

$$m_c/m_s = 11.768(33),$$

which is renormalization scheme and scale independent.

The ratio m_b/m_c has also been computed on the lattice. The most advanced calculations have been performed with $N_f = 2+1+1$ simulations [17,43,18]. Averaging these results using the FLAG [8] procedure yields

$$m_b/m_c = 4.576(11),$$

where a scale factor of $\sqrt{\chi^2/dof} = 1.45$ has been applied to the error bar. Indeed, [43] contributes 3.3 to the total χ^2.

59.5.3. *Warnings concerning the use of the pole mass* :

For an observable particle such as the electron, the position of the pole in the propagator is the definition of its mass. In QCD this definition of the quark mass is known as the pole mass. It is known that the on-shell quark propagator has no infrared divergences in perturbation theory [45,46], so this provides a perturbative definition of the quark mass. However, the pole mass cannot be used to arbitrarily high accuracy because of non-perturbative infrared effects in QCD. In fact the full quark propagator has no pole because the quarks are confined, so that the pole mass cannot be defined outside of perturbation theory. The relation between the pole mass m_Q and the $\overline{\rm MS}$ mass $\overline{m}_Q$, used throughout this review, is known to three loops [47–50]

$$\begin{aligned} m_Q = \overline{m}_Q(\overline{m}_Q)\Bigg\{1 + \frac{4\overline{\alpha}_s(\overline{m}_Q)}{3\pi} \\ + \left[-1.0414\sum_q\left(1 - \frac{4}{3}\frac{\overline{m}_q}{\overline{m}_Q}\right) + 13.4434\right]\left[\frac{\overline{\alpha}_s(\overline{m}_Q)}{\pi}\right]^2 \\ + \left[0.6527N_L^2 - 26.655N_L + 190.595\right]\left[\frac{\overline{\alpha}_s(\overline{m}_Q)}{\pi}\right]^3\Bigg\}, \end{aligned} \tag{59.20}$$

where $\overline{\alpha}_s(\mu)$ is the strong interaction coupling constants in the $\overline{\rm MS}$ scheme, and the sum over q extends over the N_L flavors lighter than Q. The complete mass dependence of the α_s^2 term can be found in [47]; the mass dependence of the α_s^3 term is not known. For the b-quark, Eq. (59.20) reads

$$m_b = \overline{m}_b\,(\overline{m}_b)\,[1 + 0.10 + 0.05 + 0.03]\,, \tag{59.21}$$

where the contributions from the different orders in α_s are shown explicitly. The two and three loop corrections are comparable in size and have the same sign as the one loop term. This is a signal of the asymptotic nature of the perturbation series (there is a renormalon in the pole mass [51]) . Such a badly behaved perturbation expansion can be avoided by directly extracting, from data, the mass defined in the $\overline{\rm MS}$ (used in this review) or other short-distance schemes (see below), without invoking the pole mass as an intermediate step.

59.6. Numerical values and caveats

The quark masses in the particle data listings have been obtained by using a wide variety of methods. Each method involves its own set of approximations and uncertainties. In most cases, the errors are an estimate of the size of neglected higher-order corrections or other uncertainties. The expansion parameters for some of the approximations are not very small (for example, they are $m_K^2/\Lambda_\chi^2 \sim 0.25$ for the SU(3) chiral expansion and $\Lambda_{\rm QCD}/m_b \sim 0.1$ for the heavy-quark expansion), so an unexpectedly large coefficient in a neglected higher-order term could significantly alter the results. Thus, before using a particular result, it is important to understand the possible limitations of the approach used to obtain it. It is also important to note that the quark mass values can be significantly different in the different schemes.

We have specified all masses in the $\overline{\rm MS}$ scheme. For light quarks, the renormalization scale has been chosen to be $\mu = 2\,{\rm GeV}$. Quoting these masses at smaller values of μ, where perturbative corrections become significantly larger, would introduce unnecessary uncertainties in the results. In fact, as lattice calculations, performed on finer and finer lattices, allow to determine quark masses, fully non-perturbatively, at larger and larger values of μ, it may become advantageous to quote quark mass results at renormalization scales above 2 GeV, where perturbative uncertainties are smaller.

The heavy quark masses obtained using HQET, QCD sum rules, or lattice gauge theory are consistent with each other if they are all converted into the same scheme and scale. For these quarks it is conventional to choose the renormalization scale equal to the quark mass, so we have quoted $\overline{m}_Q(\mu)$ at $\mu = \overline{m}_Q$ for the c and b quarks. Given the small size of the charm quark mass, in the future it may become advantageous to quote its value at larger values of μ so as not to introduce unnecessary perturbative uncertainties (see discussion above). Analyses of inclusive B meson decays have shown that other mass definitions lead to a better behaved perturbation series than for the $\overline{\rm MS}$ mass, and hence to more accurate mass values [52,53,54,56]. Thus, we have chosen to also give values for one of these, the b quark mass in the 1S-scheme [52,53]. Other schemes that have been proposed are the PS-scheme [54], the kinetic scheme [55] and, most recently, the minimal renormalon-subtracted mass (MRS) [56] used in the lattice calculation [18].

If necessary, we have converted values in the original papers to our chosen scheme using two-loop formulæ. It is important to realize that our conversions introduce significant additional errors. In converting to the $\overline{\rm MS}$ b-quark mass, for example, the three-loop conversions from the 1S and pole masses give values about 35 MeV and 135 MeV lower than the two-loop conversions. The uncertainty in $\alpha_s(M_Z) = 0.1179 \pm 0.0010$ [1] gives an uncertainty of ± 9 MeV and ± 21 MeV respectively in the same conversions. We have not added these additional errors when we do our conversions. The α_s value in the conversion is correlated with the α_s value used in determining the quark mass, so the conversion error is not a simple additional error on the quark mass.

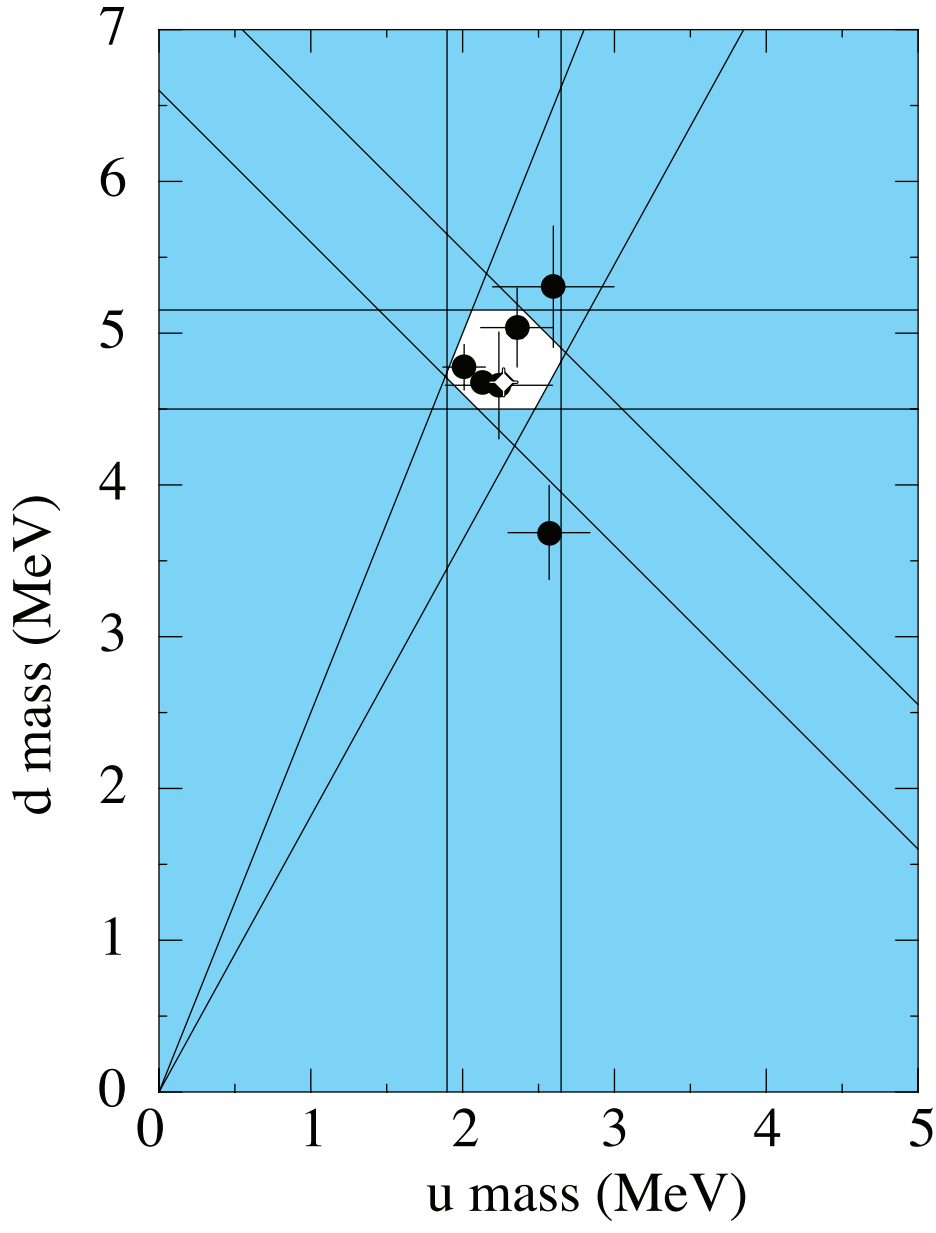

Figure 59.2: The allowed region (shown in white) for up quark and down quark masses renormalized in the $\overline{\rm MS}$ scheme at 2 GeV. This region was determined in part from papers reporting values for m_u and m_d (data points shown) and in part from an analysis of the allowed ranges of other mass parameters (see Fig. 59.3). The parameter $(m_u + m_d)/2$ yields the two downward-sloping lines, while m_u/m_d yields the two rising lines originating at (0,0). There are two overlapping data points, so one of them is shown as a white diamond (it has very small error bars).

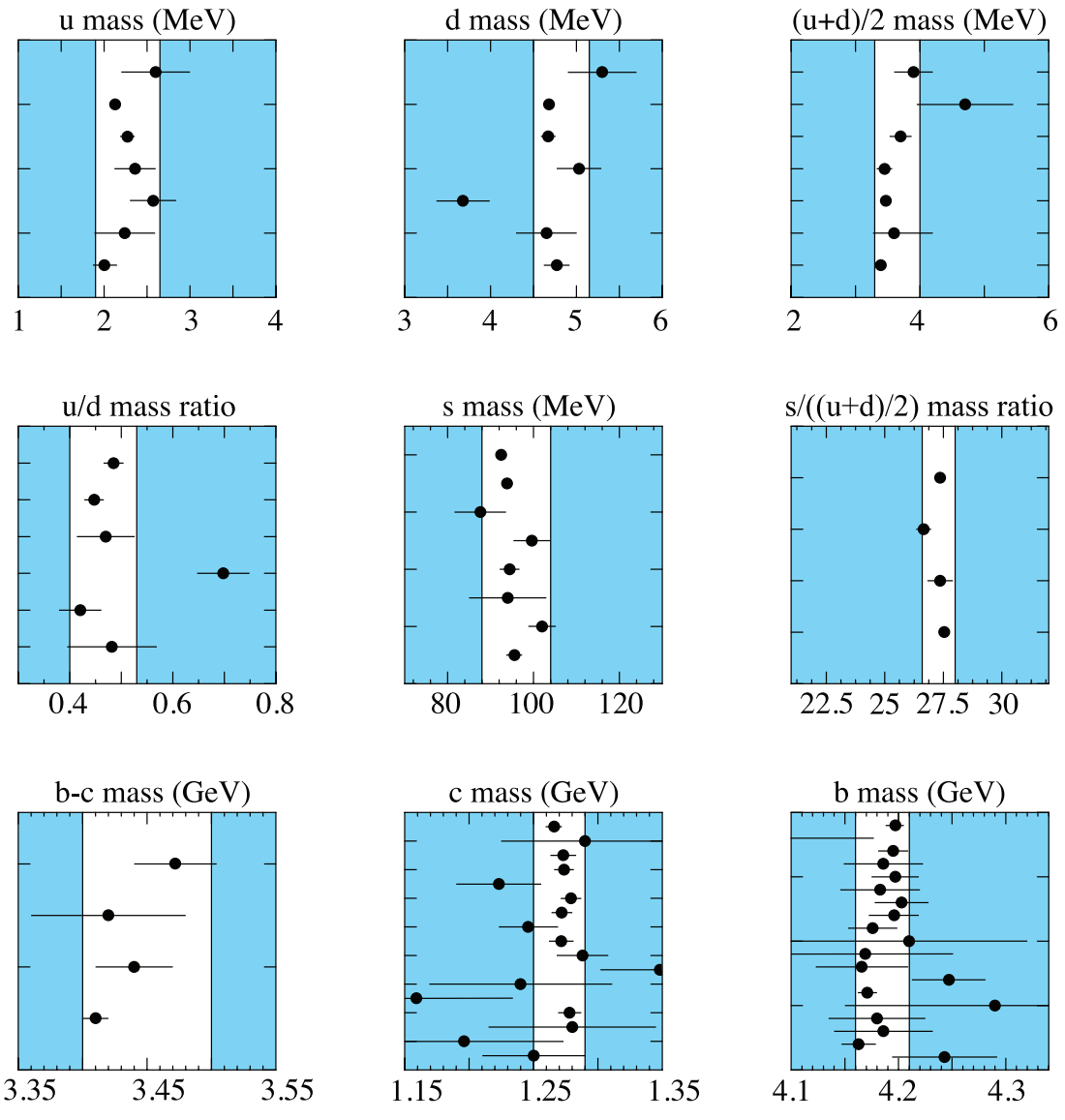

Figure 59.3: The values of each quark mass parameter taken from the Data Listings. The points are in chronological order with the more recent measurements at the top. The shaded regions indicate values excluded by our evaluations; some regions were determined in part through examination of Fig. 59.2.

References:

1. See the review of QCD in this volume..
2. A.V. Manohar and H. Georgi, Nucl. Phys. **B234**, 189 (1984).
3. K.G. Chetyrkin, Phys. Lett. **B404**, 161 (1997).
4. J.A.M. Vermaseren, S.A. Larin, and T. van Ritbergen, Phys. Lett. **B405**, 327 (1997).
5. K.G. Chetyrkin, B.A. Kniehl, and M. Steinhauser, Nucl. Phys. **B510**, 61 (1998).

6. G. Martinelli *et al.*, Nucl. Phys. **B445**, 81 (1995).
7. K. Jansen *et al.*, Phys. Lett. **B372**, 275 (1996).
8. S. Aoki *et al.* [Flavour Lattice Averaging Group], [arXiv:1902.08191 [hep-lat]].
9. P. Petreczky and J. H. Weber, arXiv:1901.06424 [hep-lat].
10. A. Bazavov *et al.* [MILC collaboration], PoS **CD09** (2009) 007.
11. A. Bazavov *et al.*, PoS **LATTICE2010** (2010) 083.
12. S. Durr *et al.*, Phys. Lett. **B701**, 265 (2011).
13. S. Durr *et al.*, JHEP **1108**, 148 (2011).
14. T. Blum *et al.* [RBC and UKQCD collaborations], Phys. Rev. **D93**, 074505 (2016).
15. Y. Maezawa and P. Petreczky, Phys. Rev. **D94**, 034507 (2016).
16. N. Carrasco *et al.* [ETM collaboration], Nucl. Phys. **B887**, 19 (2014).
17. B. Chakraborty *et al.* [HPQCD collaboration], Phys. Rev. **D91**, 054508 (2015).
18. A. Bazavov *et al.* [Fermilab Lattice and MILC and TUMQCD collaborations], Phys. Rev. **D98**, 054517 (2018).
19. A. T. Lytle *et al.* [HPQCD collaboration], Phys. Rev. **D98**, 014513 (2018).
20. S. Borsanyi *et al.*[BMW collaboration], Science **347**, 1452 (2015).
21. Z. Fodor *et al.*[BMW collaboration], Phys. Rev. Lett. **117**, 082001 (2016).
22. D. Giusti, V. Lubicz, C. Tarantino, G. Martinelli, S. Sanfilippo, S. Simula and N. Tantalo [RM123 collaboration], Phys. Rev. **D95**, 114504 (2017).
23. S. Weinberg, Physica **96A**, 327 (1979).
24. J. Gasser and H. Leutwyler, Ann. Phys. **158**, 142 (1984).
25. For a review, see A. Pich, Rept. on Prog. in Phys. **58**, 563 (1995).
26. S. Weinberg, Trans. N.Y. Acad. Sci. **38**, 185 (1977).
27. D.B. Kaplan and A.V. Manohar, Phys. Rev. Lett. **56**, 2004 (1986).
28. G. Colangelo, S. Lanz, H. Leutwyler and E. Passemar, Eur. Phys. J. C **78**, no. 11, 947 (2018).
29. S. Weinberg, Phys. Rev. Lett. **18**, 507 (1967).
30. M.A. Shifman, A.I. Vainshtein, and V.I. Zakharov, Nucl. Phys. **B147**, 385 (1979).
31. E. Braaten, S. Narison, and A. Pich, Nucl. Phys. **B373**, 581 (1992).
32. F. Le Diberder and A. Pich, Phys. Lett. **B286**, 147 (1992) doi:10.1016/0370-2693(92)90172-Z.
33. N. Isgur and M.B. Wise, Phys. Lett. **B232**, 113 (1989), *ibid*, **B237**, 527 (1990).
34. G.T. Bodwin, E. Braaten, and G.P. Lepage, Phys. Rev. **D51**, 1125 (1995).
35. A.H. Hoang, Phys. Rev. **D61**, 034005 (2000).
36. K. Melnikov and A. Yelkhovsky, Phys. Rev. **D59**, 114009 (1999).
37. M. Beneke and A. Signer, Phys. Lett. **B471**, 233 (1999).
38. B. Dehnadi, A. H. Hoang, V. Mateu and S. M. Zebarjad, JHEP **1309**, 103 (2013).
39. I. Allison *et al.* [HPQCD collaboration], Phys. Rev. **D78**, 054513 (2008).
40. C. Alexandrou, V. Drach, K. Jansen, C. Kallidonis and G. Koutsou, Phys. Rev. D **90**, no. 7, 074501 (2014).
41. J. Heitger *et al.* [ALPHA collaboration], JHEP **0402**, 022 (2004).
42. B. Colquhoun, R. J. Dowdall, C. T. H. Davies, K. Hornbostel and G. P. Lepage [HPQCD collaboration], Phys. Rev. D **91**, no. 7, 074514 (2015).
43. A. Bussone *et al.* [ETM collaboration], Phys. Rev. D **93**, no. 11, 114505 (2016).

44. P. Gambino, A. Melis and S. Simula, Phys. Rev. D **96**, no. 1, 014511 (2017).
45. R. Tarrach, Nucl. Phys. **B183**, 384 (1981).
46. A. Kronfeld, Phys. Rev. **D58**, 051501 (1998).
47. N. Gray *et al.*, Z. Phys. **C48**, 673 (1990).
48. D.J. Broadhurst, N. Gray, and K. Schilcher, Z. Phys. **C52**, 111 (1991).
49. K.G. Chetyrkin and M. Steinhauser, Phys. Rev. Lett. **83**, 4001 (1999).
50. K. Melnikov and T. van Ritbergen, Phys. Lett. **B482**, 99 (2000).
51. M. Beneke and V. M. Braun, Nucl. Phys. B **426**, 301 (1994).
52. A.H. Hoang, Z. Ligeti, A.V. Manohar, Phys. Rev. Lett. **82**, 277 (1999).
53. A.H. Hoang, Z. Ligeti, A.V. Manohar, Phys. Rev. **D59**, 074017 (1999).
54. M. Beneke, Phys. Lett. **B434**, 115 (1998).
55. P. Gambino and N. Uraltsev, Eur. Phys. J. **C34**, 181 (2004).
56. N. Brambilla *et al.* [TUMQCD collaboration], Phys. Rev. D **97**, no. 3, 034503 (2018).
57. C.T.H. Davies *et al.* [HPQCD collaboration], Phys. Rev. Lett. **104**, 132003 (2010).
58. A. Bazavov *et al.* [MILC Collaboration], Rev. Mod. Phys. **82**, 1349 (2010).
59. Y. B. Yang *et al.* [χQCD collaboration], Phys. Rev. D **92**, no. 3, 034517 (2015).